VERSITA

FeS$_2$ quantum dots sensitized nanostructured TiO$_2$ solar cell: photoelectrochemical and photoinduced absorption spectroscopy studies

I. BEDJA[*]

CRC, Department of Optometry, College of Applied Medical Sciences,
King Saud University, PO Box 10219 Riyadh, 11433 Saudi Arabia

Thin films of nanostructured TiO$_2$ have been modified with FeS$_2$ (pyrite) nano-particles by a low temperature chemical reaction of iron pentacarbonyl with sulfur in xylene. Quantum size effects are manifested by the observation of a blue shift in both absorption and photocurrent action spectra. PIA (Photoinduced absorption spectroscopy), where the excitation is provided by a square-wave modulated (on/off) monochromatic light emitting diode, is a multipurpose tool in the study of dye-sensitized solar cells. Here, PIA is used to study quantum-dot modified TiO$_2$ nanostructured electrodes. The PIA spectra obtained give evidence for long-lived photoinduced charge separation: electrons are injected into the metal oxide and holes are left behind in the FeS$_2$ quantum dot. Time-resolved PIA shows that recombination between electrons and holes occurs on a millisecond timescale. The Incident-Photon-to-Current Efficiency of about 23 % was obtained at 400 nm excitation. The performances of TiO$_2$ electrodes modified with FeS$_2$ are relatively low, which is explained by the presence of FeS$_2$ phases other than the photoactive pyrite phase, as follows from the XRD spectrum.

Keywords: *FeS$_2$, quantum-dots, TiO$_2$, nanostructures, PIA, photoelectrochemistry*

1. Introduction

Great effort is being made to obtain efficient and inexpensive organic and inorganic solar cells. The approach of using semiconductor colloids for the design of optically transparent thin semiconductor films is considered to be one of the best alternatives for the amorphous silicon solar cells. The films with a wide band gap, made from colloidal metal oxide semiconductors using this approach attract a lot of attention. This is primarily because they are quite stable and because they predominantly absorb light in the UV range. The usefulness of these systems for solar cell applications was made possible by sensitization of their semiconductor surfaces into visible regions either by organic dyes (dye sensitization) [1–4] or by inorganic short band gap semiconductors also called quantum dots (QDs) (semiconductor sensitization) [5–8]. The efficiencies of power conversion in the range of 8–12 % in diffuse day-light have been obtained by the sensitization of highly porous TiO$_2$ film with ruthenium complex based dyes [1]. On the other hand, wide band gap semiconductors have been sensitized by short band gap (quantum dots) semiconductor materials (CdS/TiO$_2$ [5], CdSe/TiO$_2$ [5], ZnS/ZnO [4]) as an alternative to dye sensitization. Vogel and coworkers [6] investigated the sensitization of nanoporous TiO$_2$, ZnO, SnO$_2$, etc. by quantum-sized CdS and PbS. Photocurrent quantum yields of up to 80 % and open circuit voltages of up to 1 V were obtained. In contrast to the dye sensitized solar cells, fundamental understanding of the factors controlling the interfacial electron transfer reactions is limited.

Short-band gap semiconductor FeS$_2$ (pyrite) is another favorable candidate for the photosensitization material because of its environmental compatibility, high stability toward photocorrosion as well as very good absorption in the visible region of the solar spectrum. Due to its favorable solid state properties [2, 3], the pyrite polymorph of iron disulfide is of particular interest, and shows promise for solar energy conversion devices in both photoelectrochemical and photovoltaic solar cells [5] as well as

solid state solar cells [6]. Ennaoui et al. [9] reported on an interesting photoresponse of a TiO_2 electrode modified with FeS_2 using CVD method. Jing H. Fang et al. have recently [10] reported a method (similar to that described by Chatzitheodorou [11]) of modification of the wide band gap TiO_2 (Degussa P25) by quantum sized FeS_2 particles.

In this work, modification of TiO_2 metal oxide nanostructured films by quantum dots FeS_2 is reported which is similar to the method described previously by Chatzitheodorou [11] on TiO_2 films but with minor changes. The results describe the photoelectrochemical properties and photoinduced absorption spectroscopy of TiO_2 modified with FeS_2 quantum dots.

2.   Experimental

2.1.   Preparation of nanostructured TiO_2 films

Deposition of the TiO_2 paste (from EPFL, Switzerland) on a flat FTO substrate is accomplished in a very fast and reproducible manner by the *doctor-blade* method. In this method, the substrate electrode (8 mm × 30 mm) is taped down at the edges onto a flat surface between two parallel pieces of FTO glass of the same thickness, using 3M Scotch™ tape. A droplet of the TiO_2 paste is spread out homogeneously over the substrate, with the Scotch tape determining the thickness and serving as the boundary. After removal of the tape, the films are heated at 125 °C in air for 6 min. The process is repeated 3–4 times and then the sample is annealed at 450 °C for 30 min. During this annealing step, the solvent and organic additives are removed, while the TiO_2 nanoparticles become interconnected. Slow cooling yields 5–6 μm thick crack-free nanostructured TiO_2 films. Before the conducting glass (ITO) was coated with TiO_2, a layer called the blocking area, which consisted of much smaller TiO_2 nanoparticles than those forming the substrate, was deposited on the ITO plate. This layer blocked the electrolyte from reaching the ITO electrode to prevent short circuits. ITO plates were put into 0.02 M $TiCl_4$ solution and kept at 70 °C for 30 min. Then the final TiO_2-NP films (thickness

5–6 μm) were made on top of the blocking layer as described earlier [12]. The working electrodes were then sintered at 450 °C for 30 min using a heat gun, and cooled down to room temperature.

2.2.   Surface modification of TiO_2 by FeS_2 quantum dots

Modification of TiO_2 metal oxide nanostructured films by FeS_2 quantum dots was made by a method similar to the method described previously by Chatzitheodorou [11] with minor changes. The clean TiO_2 electrode was put into the solution of sulfur (0.02 M) in xylene, followed by immersion of iron pentacarbonyl (0.01 M) in xylene at a temperature close to 139 °C. The whole experiment was carried out under a nitrogen atmosphere. This procedure was repeated several times. The structure and morphology of the films were examined using X-ray diffraction (Siemens D5000) and scanning electron microscopy (LEO 1550 EDS), respectively.

2.3.   Characterization Methods

UV-Vis spectra were recorded using a Hewlett-Packard 8453 diode array spectrometer. The photoelectrochemical measurements were carried out in a quartz cell similar to that in Fig. 1 [16] equipped with two electrodes consisting of a reference (Ag/AgCl) and a counter (Pt wire) electrode. Princeton Applied Research (PAR) Models 173 and 175 universal potentiostats were used in electrochemical measurements.

For PIA spectroscopy (see the setup described in ref. [12]), excitation of the sample was provided by light from a blue LED (Luxeon Star 1 W, Royal Blue, 470 nm), which was square-wave modulated (on/off) by electronic means using an HP 33120A waveform generator and a home-built LED driver system. The beam with intensity in the range of 0.5–30 mW cm^{-2}, excited a sample area of about 1 cm^2. White probe light was provided by a 20 W tungsten-halogen lamp. A cutoff filter (Schott RG715) was used to minimize the excitation of the sample by the probe light. The transmitted probe light was focused onto a monochromator (Acton Research Corporation SP-150) and detected using a UV-enhanced Si photodiode, connected to a lock-in amplifier
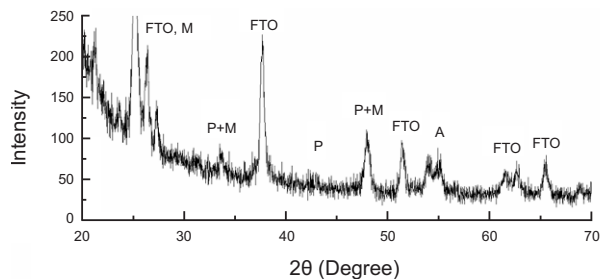
*FeS$_2$ quantum dots sensitized nanostructured TiO$_2$ solar cell: photoelectrochemical and photoinduced
absorption spectroscopy studies*

173

Fig. 1. XRD spectrum of TiO$_2$ nanoparticulate film after FeS$_2$ deposition: A = Anatase; P = Pyrite; M = Marcasite.

via a current amplifier (Stanford Research Systems models 830 and 570, respectively). For the time-resolved studies the output of the current amplifier was connected to a data acquisition board (National Instruments PCI-6052E). All PIA measurements were carried out at room temperature.

3. Results and discussion

3.1. XRD and SEM

The XRD spectrum (Fig. 1) of TiO$_2$ film modified with FeS$_2$ particles shows, in addition to TiO$_2$ anatase peaks, FeS$_2$ peaks which appear to have multiple phases namely cubic (pyrite: P) and orthorhombic marcasite (M).

Fig. 2 shows a SEM picture of the surface morphology of a TiO$_2$ nanostructured film on a conducting glass substrate. It is clear that the TiO$_2$ film is microporous and is composed of interconnected particles and pores which are uniformly distributed and have an average width of particles of about 20–30 nm. In the inset, a SEM picture of the TiO$_2$ particulate film modified with FeS$_2$ particles is shown. There are many fine particles which consist of aggregated clusters formed within the pores of TiO$_2$ film. In a similar synthesis done by Chatzitheodorou et al. [11] and Fang et al. [10], the size of the FeS$_2$ particles ranged from 20 to 50 nm. Since the TiO$_2$ microporous film possesses a larger inner surface than an outer surface, it is logical that most of the FeS$_2$ particles are formed and maintained in the pores. It was estimated in previous studies [10] that the size of the FeS$_2$ particles before aggregation is about 8 nm.
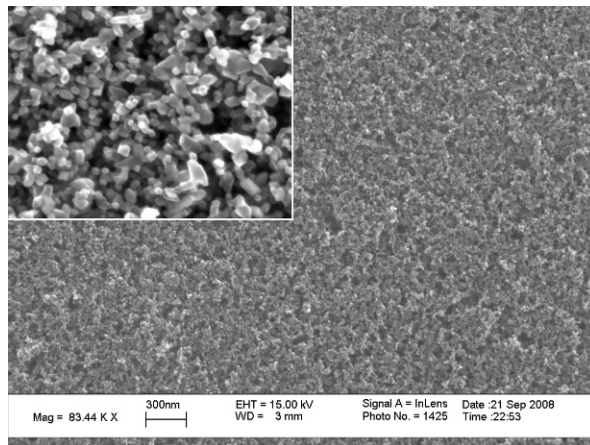

Fig. 2. SEM picture of top TiO$_2$ nanostructured film. The inset is a SEM picture of top TiO$_2$ particulate film after FeS$_2$ deposition.

3.2. Absorption and IPCE Spectra

The absorption spectra of TiO$_2$ film before and after modification with FeS$_2$ are shown in Fig. 3. A conducting glass support (FTO) was used as a reference in the measurement. The plot denoted as Fig. 3a shows the absorption spectrum of an electrode made of a nanoparticulate TiO$_2$ film while the plots 3 b–d depict the absorption spectra of TiO$_2$ films modified with FeS$_2$ at different numbers of coatings. The band gap of a TiO$_2$ rutile is 3 eV, whereas that of anatase is 3.2 eV, which corresponds to a fundamental absorption edge of 413 and 388 nm, respectively. So, the bare TiO$_2$ film, here, exhibits the fundamental absorption edge of anatase as it could be expected for TiO$_2$ paste prepared by the EPFL procedure.

The low energy tail of the 3 b–d plots comes predominately from large FeS$_2$ particles. However, the high energy absorption shoulder originates mainly from the ultra small particles. The band gap of the FeS$_2$ deposited on TiO$_2$ films was analyzed by plotting the square root of the absorbance versus photon energy (inset in Fig. 3). A linear relation was found for the square root of the absorbance, which suggests that the lowest band gap transition is indirect. The band gap, obtained by extrapolation, is about 1.6 eV. The reported value for the band gap of bulk FeS$_2$ is of 0.95 eV [9]. This suggests that
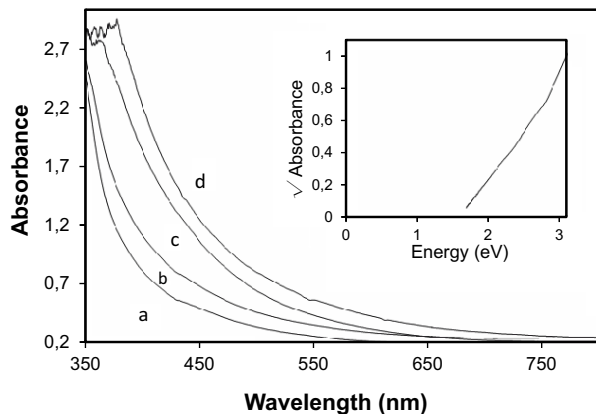
Fig. 3. Absorption spectra of (a) TiO_2 electrode made of particulate film (b) (c) (d) electrodes of TiO_2 film with different FeS_2 coating layers. All electrodes have similar thicknesses of about 6 μm. All absorption spectra use a conducting glass FTO as a reference. The inset shows a plot of (absorbance)$^{1/2}$ versus photon energy, for determination of the indirect band gap.
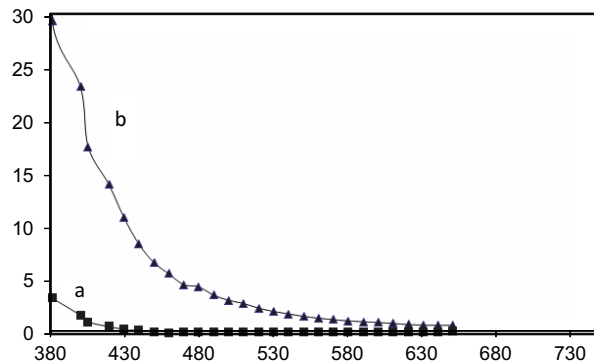

Fig. 4. (a) Incident photon-to-current conversion efficiencies (IPCE) of TiO_2 particulate photoelectrode and (b) quantum dots FeS_2 adsorbed on TiO_2 photoelectrode. (electrolyte Na_2S 0.1 M, Na_2SO_4 0.01 M).

there is a strong quantum-size effect occurring in the FeS_2 particles, otherwise, we would expect a large wavelength absorption onset near IR. This can be explained in terms of a quantum size effect of very small FeS_2 particles which causes the band gap energy to rise.

The photoelectrochemical response of the TiO_2 electrode, before and after the modification with FeS_2, was evaluated by measuring the photocurrent of the electrode at various excitation wavelengths. The incident photon-to-photocurrent efficiency (IPCE) was then determined from the expression (1) where I_{sc} is the short-circuit current (A/cm^2), I_{inc} is the incident light intensity (W/cm^2), and λ is the excitation wavelength (nanometers).

$$IPCE(\%) = 100 \cdot (1240 \cdot I_{sc})/(I_{inc}\lambda) \qquad (1)$$

Maximum IPCE obtained with this cell is about 23 % at 400 nm excitation. The onset of photocurrent of TiO_2 based electrode is seen at wavelengths below 420 nm. The photoresponse of TiO_2 electrode (Fig. 4a) has been extended to the visible range after FeS_2 modification (Fig. 4b). Although the FeS_2/TiO_2 electrode shows a visible absorption in

wavelengths longer than 580 nm, no photoresponse was detected at these wavelengths. This suggests that only the small quantum-sized FeS_2 particles play a dominant role in the spectral sensitization of TiO_2 particles, while the larger particles have little or no contribution. The reduced IPCE measured is partly due to the presence of large pores seen in the TiO_2 morphology which has helped in the aggregation of the ultra fine FeS_2 particles inside the pores. This might increase the chance of recombination of excited electrons in FeS_2 particles with the holes. This low performance can also be partially explained by a high density of surface defects, but also the unusually low open circuit voltage of 200 mV, measured previously, suggests that phase purity may also play an important role [9, 13]. Orthorhombic marcasite FeS_2 and hexagonal troilite FeS are both common iron sulfur phases (see XRD spectrum in Fig. 1), but because they have much smaller band gaps (0.34 eV for marcasite and 0.04 eV for troilite), even trace amounts of impurities would explain the low open circuit voltage observed in the previous work. The other reason for such a reduced performance may be explained by the presence of FeS_2 phases other than the photoactive pyrite phase, as follows from the XRD spectrum. Therefore, looking for a pure and stoichiometric pyrite will be very promising for solar cells based on quantum dot semiconductors.
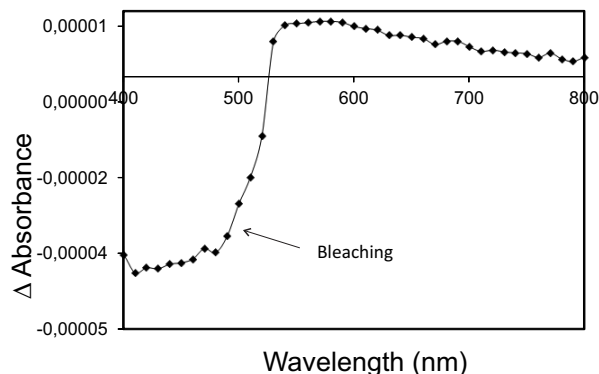
Fig. 5. Photoinduced absorption (PIA) spectrum of TiO$_2$ electrode modified by FeS$_2$ quantum dots in air. The spectrum was recorded using blue light (460 nm) excitation (42 mW$\cdot$cm^{-2}) with a modulation frequency of 9 Hz.

3.3. Photoinduced absorption spectroscopy (PIA)

3.3.1. PIA spectrum

Fig. 5 shows a typical PIA spectrum of TiO$_2$ modified with FeS$_2$ in the absence of the redox electrolyte (in air). The PIA spectrum clearly reflects the differential absorption (ΔA) spectrum of FeS$_2$ upon injection of electrons into TiO$_2$ (shown by differential absorption ΔA at large wavelengths), with a bleach of the ground state at the main absorption around 470 nm and absorption peaks at 570 nm. The remaining holes in FeS$_2$ absorb light and because the valence band electrons are missing, an apparent increase in the band gap is observed (bleaching, Moss-Burstein shift). The obtained PIA spectra give evidence for long established photoinduced charge separation: electrons are injected into the metal oxide and holes are left behind in the FeS$_2$ quantum dot.

3.3.2. PIA kinetics

The study of the kinetics in semiconductor sensitized solar cells cannot only be done by laser flash photolysis but it is also possible using time-resolved PIA measurements. Fig. 6 shows an example of such PIA transient, here with the decay recorded at 800 nm. It is clear that the recombination yield between the electrons generated in TiO$_2$ and holes generated in FeS$_2$ does not follow simple first or
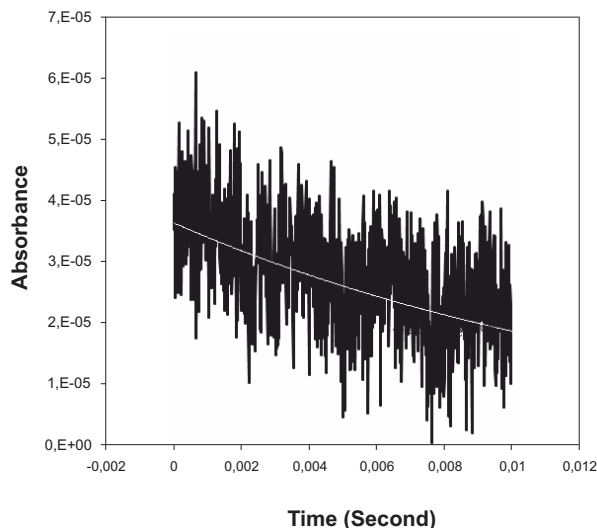

Fig. 6. PIA Transient Absorption spectrum of TiO$_2$ electrode modified by FeS$_2$ quantum dots after excitation with blue light (11 mW/cm^2) recorded at 800 nm, using a sampling rate of 10^3 s^{-1} and averaged 100 times.

even second order kinetics, but is characterized by a range of recombination times. This has been explained by the trapping of electrons within the TiO$_2$ nanocrystals [14, 15]. It is presumed that the aforementioned result could be explained by the transport of electrons through TiO$_2$ nanocrystals. For solar cell performance the (pseudo-) first-order rate constant under steady-state conditions is a relevant parameter as it can give direct information on possible recombination losses due to the reaction of electrons with holes. The analysis of the decay in Fig. 6 during the first 1 ms (using a sampling rate of 1 MHz) gives an electron-hole recombination lifetime of 6 ms. This relatively fast decay proves at least a good pore filling of the TiO$_2$ film by the ultra fine particles of pyrite. In the best TiO$_2$ based dye sensitized solar cell (DSC) using dye cis-Ru(dcbpy)2(NCS)2 (=N719, Solaronix, Switzerland), the electron-hole recombination lifetime, measured using PIA spectroscopy, was about 11 ms. [12] This analysis is, however, oversimplified as it does not take into account the much higher electron concentration present in the TiO$_2$ under the operating conditions. More detailed analysis of these losses under the presence of electrolyte should be the subject of future work with this system.

4. Conclusion

The pyrite polymorph of iron disulfide (FeS$_2$) shows promise for solar energy conversion devices in photoelectrochemical solar cells. Photoinduced absorption spectroscopy has certain advantages over laser flash photolysis, namely that experimental conditions can be kept close to typical solar cell operating conditions, its suitability to monitor slow processes and much lower cost compared to laser flash photolysis. The low performance of the FeS$_2$/TiO$_2$ electrode is mainly due to the presence of multiphase FeS$_2$. An electron-hole recombination lifetime of 6 ms, found using PIA, is comparable to that of 11 ms, found in TiO$_2$ based DSC using N719 dye. Discovering a pure and stoichiometric pyrite (free of FeS$_2$ multiphase) will be very promising for solar cells based on quantum dot semiconductors.

References

[1] O'REGAN B., GRÄTZEL M., *Nature*, 353, (1991), 737.

[2] BEDJA I., HOTCHANDANI S., KAMAT P.V., *J. Phys. Chem.*, 98, (1994), 4133.

[3] BEDJA I., HOTCHANDANI S., KAMAT J., *Appl. Phys.*, 80, (1996), 8.

[4] HEIMER T.A., HEILWEIL E.J., BIGNOZZI C.A., MEYER, G.J., *J. Phys.Chem. A*, 104, (2000), 4256.

[5] LIU D., KAMAT P.V., *J. Electrochem. Soc.*, 142, (1995), 835.

[6] VOGEL R., HOYER P., WELLER H., *J. Phys. Chem.*, 98, (1994), 3183.

[7] RABANI J., *J. Phys. Chem.*, 93, (1989), 7707.

[8] BEDJA I., HOTCHANDANI S., KAMAT P.V., *J. Berichte Der Bunsen-Gesselschaft-Physical Chemistry Chemical Physics*, 101, (1997), 1651.

[9] ENNAOUI S., FIECHTER H., PETTENKOFER CH., ALONSO-VANTYE N., BUEKER K., BRONOLD M., HOEPFNER CH., TRIBUTSCH H., *Solar Energy Materials and Solar Cells*, 29, (1993), 289.

[10] FANG H.F., WU J.W., SU L.Y., ZHANG X.Y., LU Z.H., *Chemistry Letters*, 149, (1997), 150.

[11] CHATZITHEODOROU G., FIECHTER S., KUNST M., LUCK, J., TRIBUTSCH H., *Mat. Res. Bull.*, 23, (1988), 1261.

[12] BOSCHLOO G., HAGFELDT A., *Inorganica Chemica Acta*, 361, (2008), 729.

[13] LUTHER G., *Geochim. Cosmochim. Acta*, 55, [10], (1991), 2839.

[14] HAQUE S.A., TACHIBANA Y., KLUG J.R., DURRANT D.R., *J. Phys. Chem. B*, 102, (1998), 1745.

[15] NELSON J., HAQUE S.A., KLUG D.R., DURRANT J.R., *Phys. Rev. B*, 63, (2001), 205321.

[16] BEDJA I., *Photophysics and Photoelectrochemistry Studies on Nanocrystalline Semiconductor Systems. Mechanistic studies of Photosensitization and Modulation of Electron Transfer Kinetics*, PhD. Thesis, Unversity of Quebec at Trois-Rivieres, Quebec, Canada, (1996).